Determination of electron orbital magnetic moments in carbon nanotubes

E. D. Minot, Yuval Yalsh, Vera Sazonova & Paul L. McEuen

Laboratory of Atomic and Solid-State Physics, Cornell University, Ithaca, New York, USA

presented by Dana Darau, Uni Regensburg

Contents

Motivation

States near the energetic bandgap of a CNT are predicted to have an orbital magnetic moment μ_{orb}:

- due to the motion of the electrons around the circumference of the nanotube

Motivation

States near the energetic bandgap of a CNT are predicted to have an orbital magnetic moment μ_{orb}:

- due to the motion of the electrons around the circumference of the nanotube
- much larger than the Bohr magneton μ_{B}

Motivation

States near the energetic bandgap of a CNT are predicted to have an orbital magnetic moment μ_{orb}:

- due to the motion of the electrons around the circumference of the nanotube
- much larger than the Bohr magneton μ_{B}
- thought to play a role in
  - the magnetic susceptibility of CNTs
  - the magnetoresitance observed in large MWCNTs

Motivation

States near the energetic bandgap of a CNT are predicted to have an orbital magnetic moment μ_{orb}:

- due to the motion of the electrons around the circumference of the nanotube
- much larger than the Bohr magneton μ_{B}
- thought to play a role in
  - the magnetic susceptibility of CNTs
  - the magnetoresitance observed in large MWCNTs

Electrical measurements were needed to confirm quantitatively the predicted values for μ_{orb}.

Bandstructure of a CNT without magnetic field

Graphene:

- zero-bandgap semiconductor/semimetal
- valence and conduction states meet at two points in k-space, $\mathbf{K}_1$ and $\mathbf{K}_2$

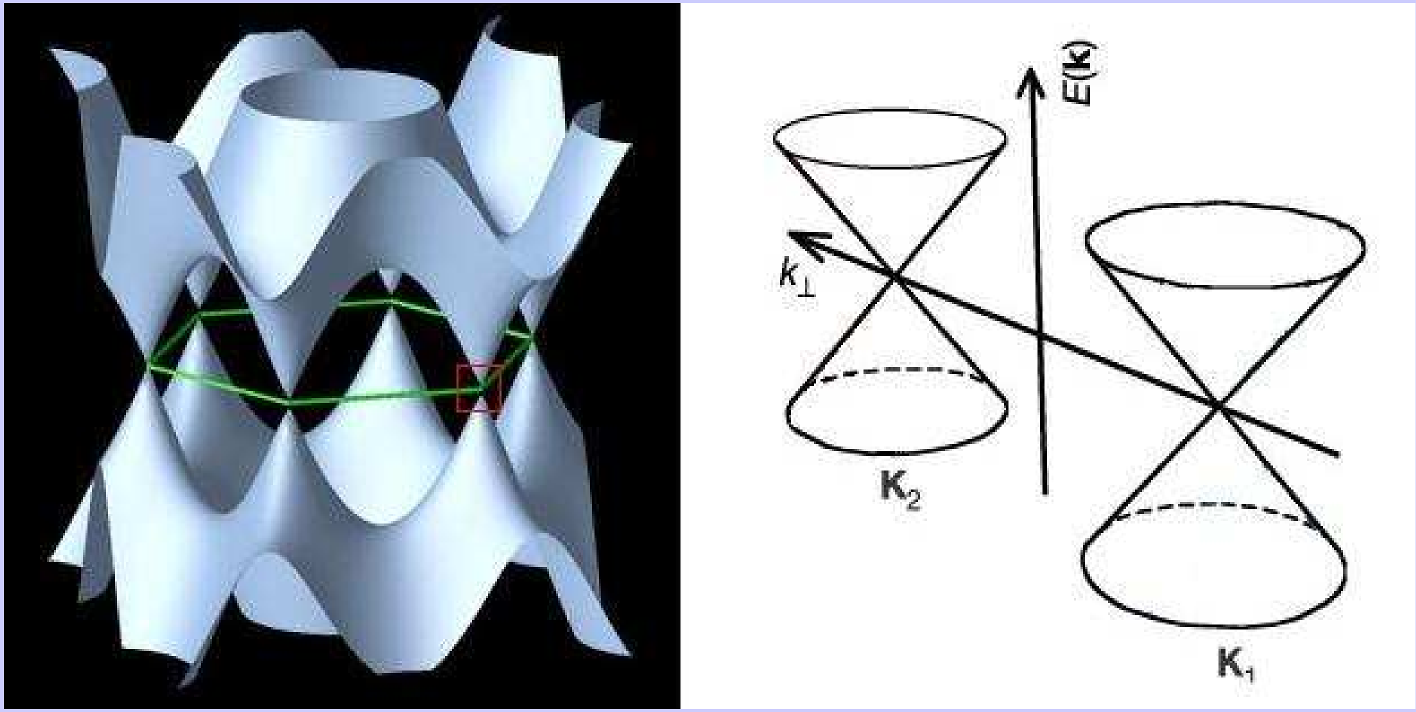

Bandstructure of a CNT without magnetic field

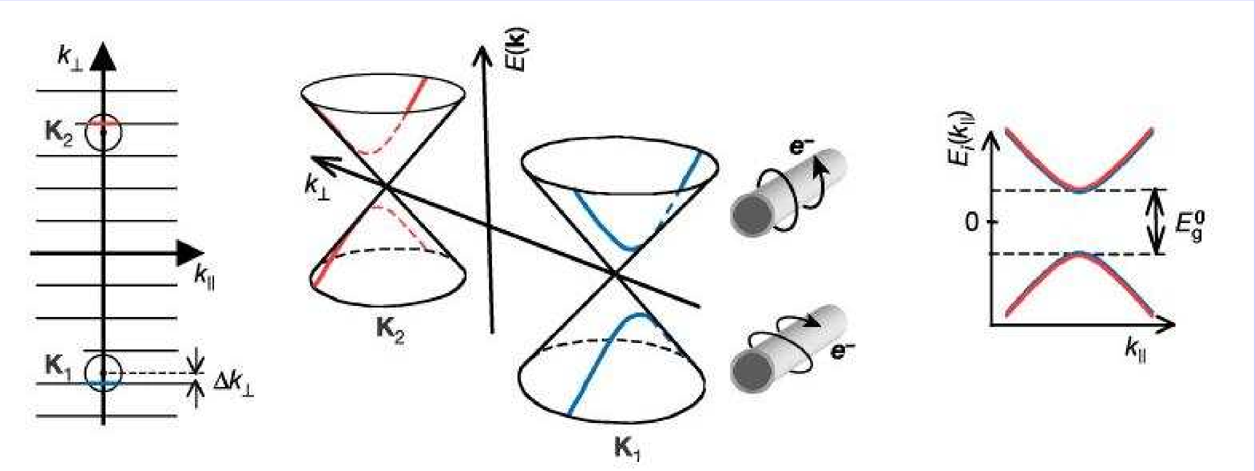

- Boundary condition

  $k_\perp = 2j/D$, D=Diameter

Bandstructure of a CNT without magnetic field

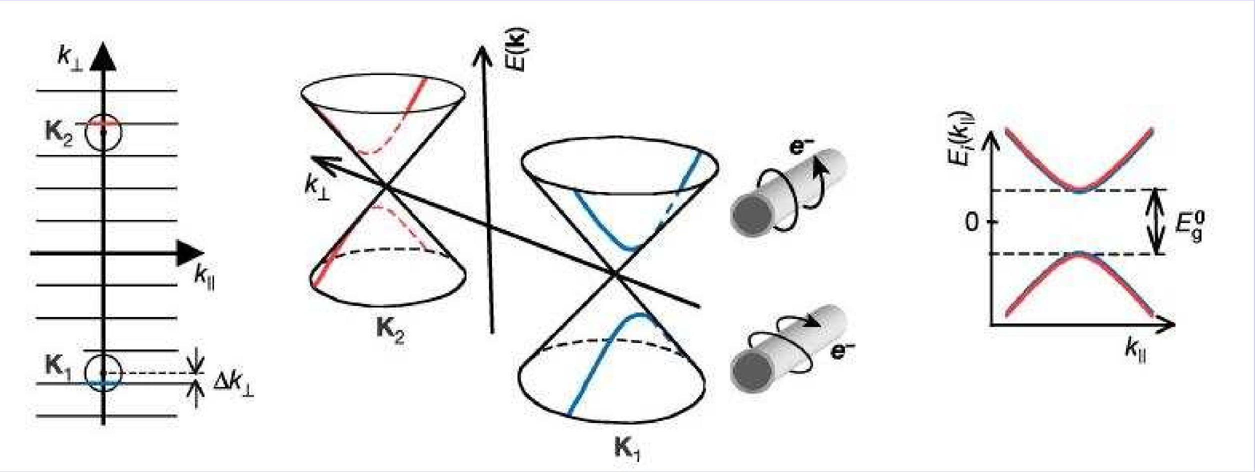

- Boundary condition

  $k_\perp = 2j/D$, D=Diameter
- Energy gap $E_\mathrm{g}^0 = \hbar v_\mathrm{F} \Delta k_\perp$

Depending on:

$\longrightarrow$ chirality

$\longrightarrow$ curvature

$\longrightarrow$ axial strain

$\longrightarrow$ twist etc.

Bandstructure of a CNT without magnetic field

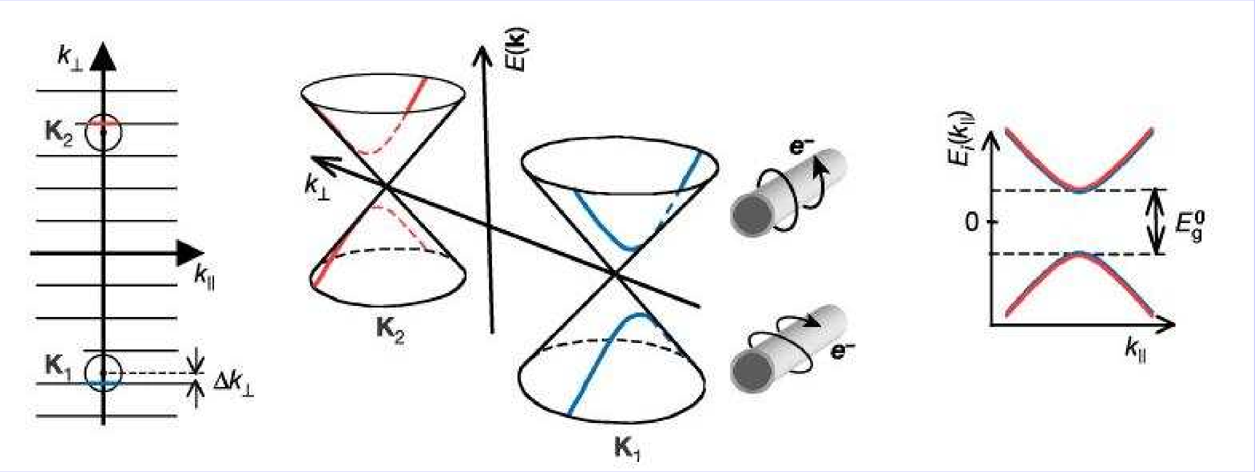

- Boundary condition

  $k_\perp = 2j/D$, D=Diameter

- Energy gap $\quad E_\mathrm{g}^0 = \hbar v_\mathrm{F} \Delta k_\perp$

- Perpendicular component of orbital velocity

  $v_\perp = (1/\hbar)(dE/dk)|_{k_\perp}$

Sense of orbit

$\longrightarrow$ clockwise (CW)
if $v_\perp > 0$

$\longrightarrow$ anticlockwise (ACW)
if $v_\perp < 0$

Bandstructure of a CNT with magnetic field

- Magnetic moment of electron states at the bandedge:

  $$\mu_{\mathrm{orb}} = \frac{eDv_\perp}{4}, \quad D\text{=Diameter}$$

  directed along the tube axis

Bandstructure of a CNT with magnetic field

- Magnetic moment of electron states at the bandedge:

$$\mu_{\mathrm{orb}} = \frac{eDv_\perp}{4},\ D\text{=Diameter}$$

directed along the tube axis

- Applied magnetic field parallel to the CNT axis shifts the energy of these states:

$$\Delta E = -\overrightarrow{\mu}_{\mathrm{orb}} \cdot \overrightarrow{B} = \pm\frac{eDv_\perp B_\parallel}{4}$$

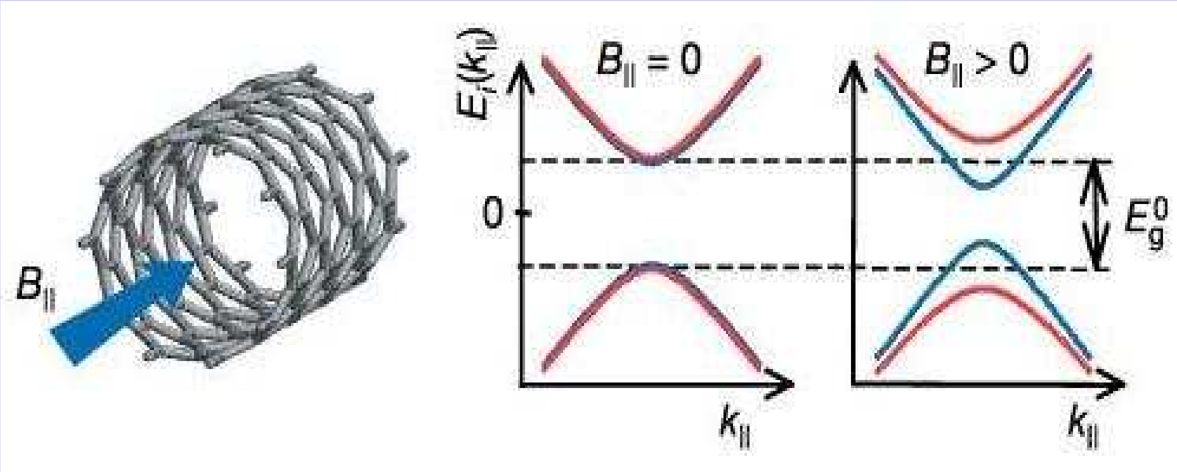

Experimental setup: Device geometry

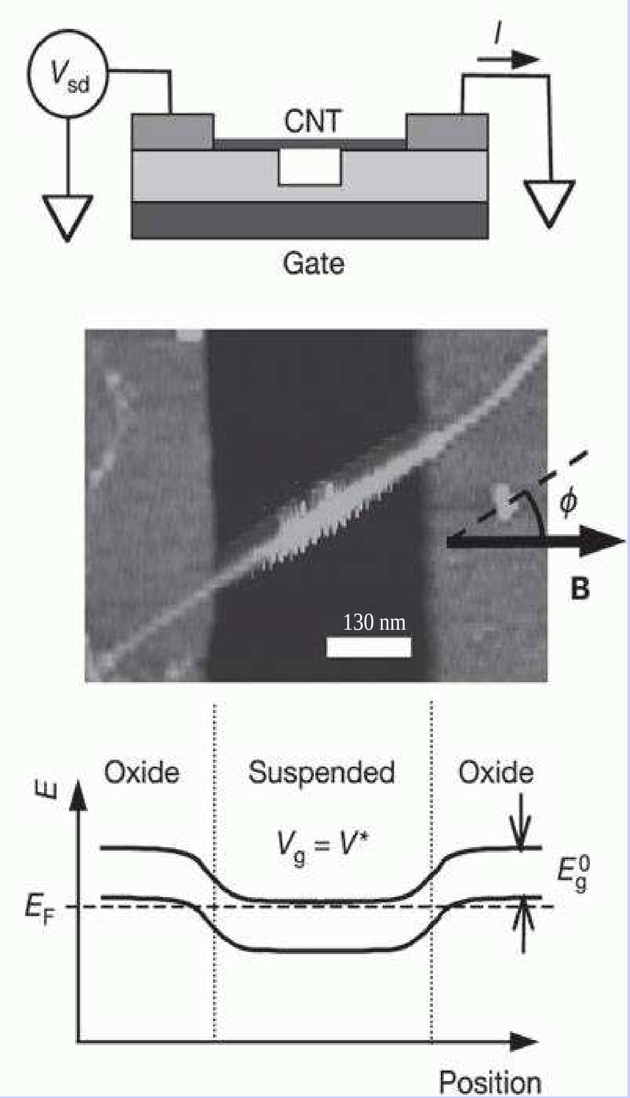

- CNT grown on Si/SiO_x
- Electrodes: 5 nm Cr, 50 nm Au
- Suspended segment:
  - L=500 nm
  - Diameters:
    - $\rightarrow$ 2.6$\pm$0.3 nm Device 1
    - $\rightarrow$ 5.0$\pm$0.3 nm Device 2
- Angle ϕ between applied magnetic field and the CNT

Thermally activated transport through charge-depleted CNTs

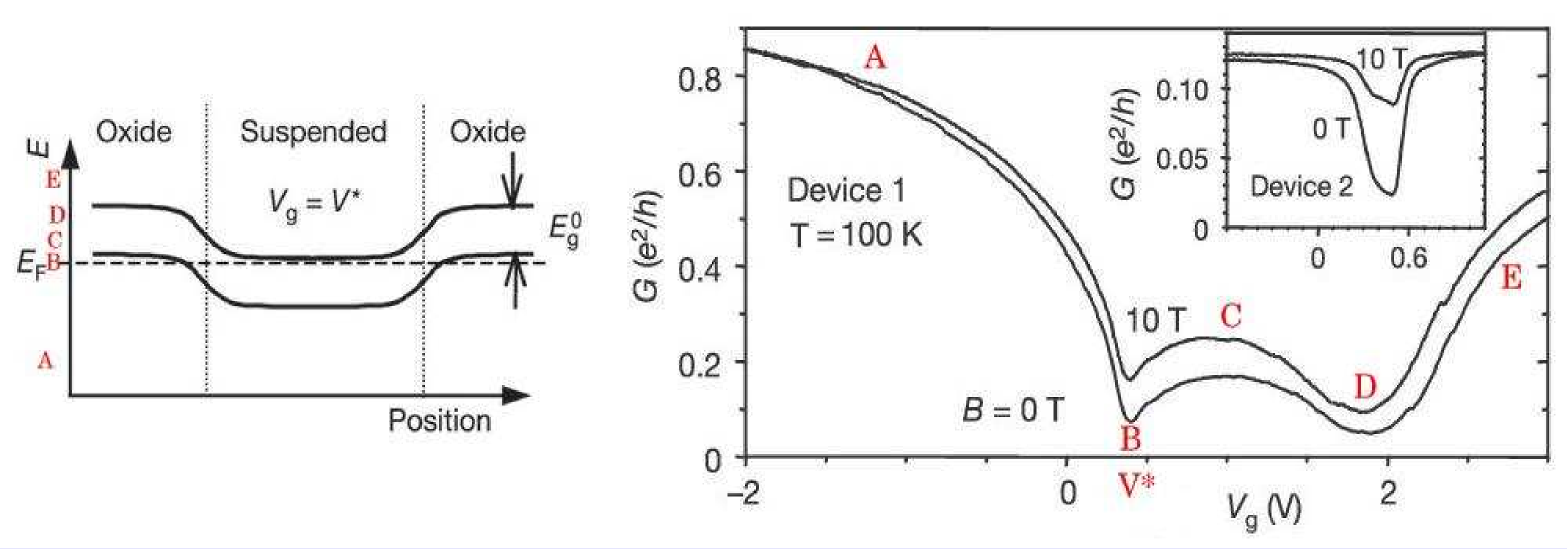

Measurements with gold-coated AFM:

- $V_g = 0$:
  - $\longrightarrow$ oxide-bound segments p-type doped
  - $\longrightarrow$ suspended section almost intrinsic

Thermally activated transport through charge-depleted CNTs

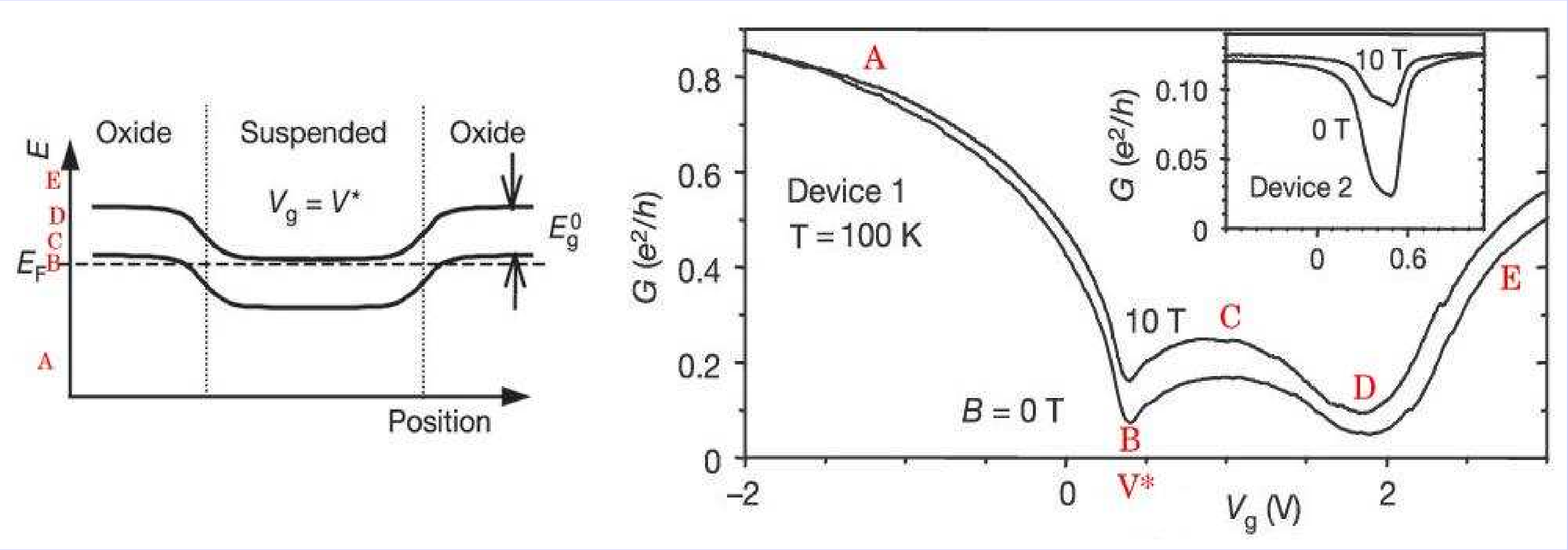

Measurements with gold-coated AFM:

- $V_g = 0$:
  - $\longrightarrow$ oxide-bound segments p-type doped
  - $\longrightarrow$ suspended section almost intrinsic
- $V_g = V^*$, V_g small:
  - $\longrightarrow$ number of thermally activated charge carriers in suspended section minimized
  - $\longrightarrow$ conductance occurs via thermal activation across the energy gap

Thermally activated transport through charge-depleted CNTs

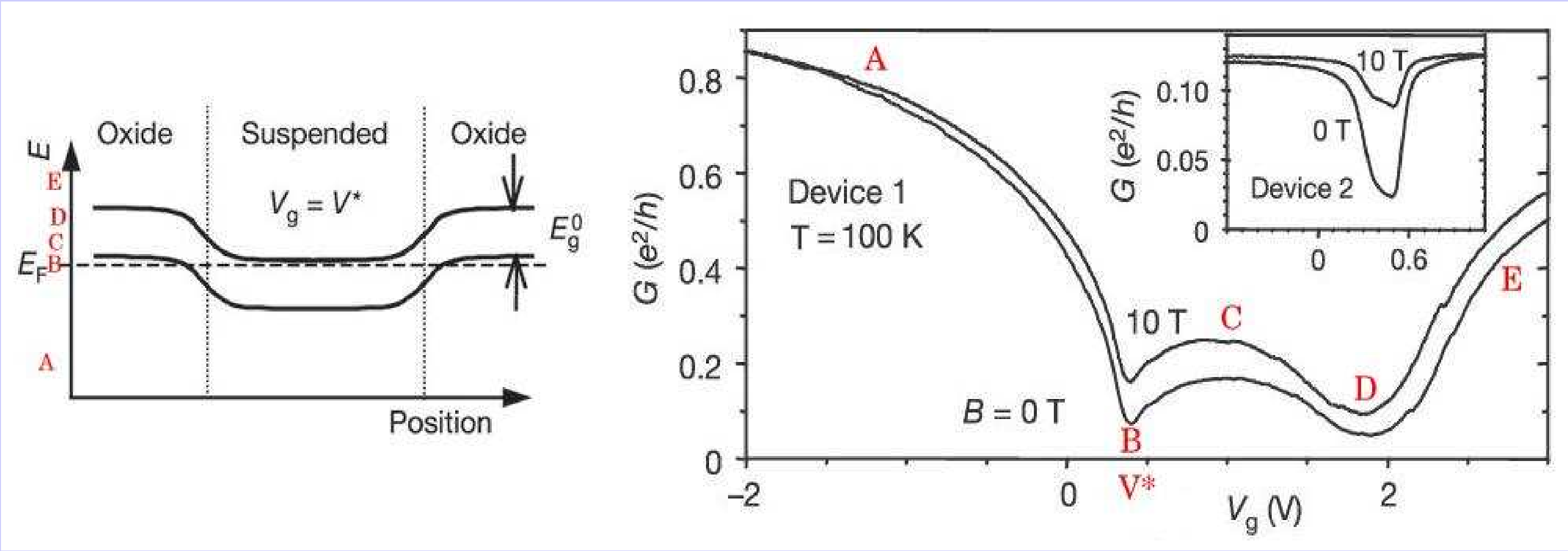

Measurements with gold-coated AFM:

- $V_{\mathrm{g}} = 0$:
  - $\longrightarrow$ oxide-bound segments p-type doped
  - $\longrightarrow$ suspended section almost intrinsic
- $V_{\mathrm{g}} = V^*$, V_{g} small:
  - $\longrightarrow$ number of thermally activated charge carriers in suspended section minimized
  - $\longrightarrow$ conductance occurs via thermal activation across the energy gap

Addition of magnetic field substantially increases the conductance around $V_{\mathrm{g}} = V^*$.

Thermally activated transport through charge-depleted CNTs

$G_{\mathrm{susp}}(V^*)$ = Minimum conductance due to thermal activation

Fermi-Dirac: $$f_{1,2}(E) = \frac{1}{\exp\left(\frac{E \pm \frac{eV}{2} - E_{\mathrm{F}}}{k_{\mathrm{B}}T}\right) + 1}$$

Landauer: $$I = \frac{2e}{h} \int T(E)[f_1(E) - f_2(E)]$$

$$G = \partial I / \partial V$$

Thermally activated transport through charge-depleted CNTs

$G_{\mathrm{susp}}(V^*)$ = Minimum conductance due to thermal activation

Fermi-Dirac: $$f_{1,2}(E) = \frac{1}{\exp\left(\dfrac{E \pm \frac{eV}{2} - E_{\mathrm{F}}}{k_{\mathrm{B}}T}\right) + 1}$$

Landauer: $$I = \tfrac{2e}{h} \int T(E)[f_1(E) - f_2(E)]$$

$$G = \partial I / \partial V$$

$$\Longrightarrow G_{\mathrm{susp}}(V^*, T) = \frac{2e^2}{h} \sum_{i=1,2} |t_i|^2 \frac{2}{\exp(E_{\mathrm{g}}^{K_i}/k_{\mathrm{B}}T) + 1}$$

Thermally activated transport through charge-depleted CNTs

$G_{\mathrm{susp}}(V^*)$ = Minimum conductance due to thermal activation

Fermi-Dirac: $$f_{1,2}(E) = \frac{1}{\exp\left(\dfrac{E \pm \dfrac{eV}{2} - E_{\mathrm{F}}}{k_{\mathrm{B}}T}\right) + 1}$$

Landauer: $$I = \tfrac{2e}{h} \int T(E)[f_1(E) - f_2(E)]$$

$$G = \partial I / \partial V$$

$$\Longrightarrow G_{\mathrm{susp}}(V^*, T) = \frac{2e^2}{h} \sum_{i=1,2} |t_i|^2 \frac{2}{\exp(E_{\mathrm{g}}^{K_i}/k_{\mathrm{B}}T) + 1}$$

Device resistance: $$G^{-1} = G_{\mathrm{susp}}^{-1} + \underbrace{G_{\mathrm{p}}^{-1} + G_{\mathrm{contact}}^{-1}}_{\text{largely T-independent}}$$

Thermally activated transport through charge-depleted CNTs

$G_{\mathrm{susp}}(V^*)$ = Minimum conductance due to thermal activation

Fermi-Dirac: $$f_{1,2}(E) = \frac{1}{\exp\left(\frac{E \pm \frac{eV}{2} - E_{\mathrm{F}}}{k_{\mathrm{B}}T}\right) + 1}$$

Landauer: $$I = \tfrac{2e}{h} \int T(E)[f_1(E) - f_2(E)]$$

$$G = \partial I / \partial V$$

$$\Longrightarrow G_{\mathrm{susp}}(V^*, T) = \frac{2e^2}{h} \sum_{i=1,2} |t_i|^2 \frac{2}{\exp(E_{\mathrm{g}}^{K_i}/k_{\mathrm{B}}T) + 1}$$

Device resistance: $$G^{-1} = G_{\mathrm{susp}}^{-1} + \underbrace{G_{\mathrm{p}}^{-1} + G_{\mathrm{contact}}^{-1}}_{\text{largely T-independent}}$$

$\longrightarrow$ To plot: $$\Delta R(T) = G(V^*, T)^{-1} - G(V_{\mathrm{g}} \ll 0, T)^{-1}$$

Thermally activated transport through charge-depleted CNTs

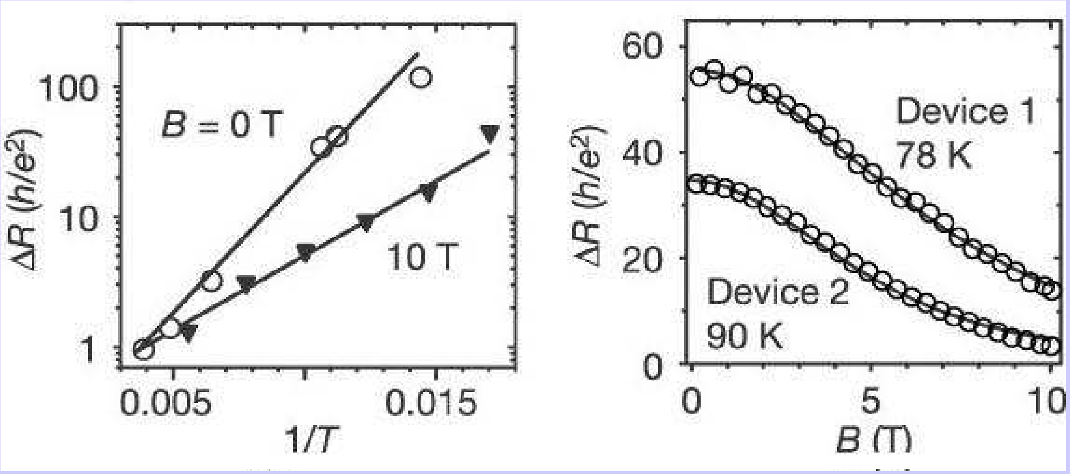

Device 2:

- $\boldsymbol{B} = 0$: $\quad E_g^0 = 40$ meV
  $|t_1|^2 + |t_2|^2 = 1.6 \quad \Longrightarrow$ two channels, nearly ballistic transport

Thermally activated transport through charge-depleted CNTs

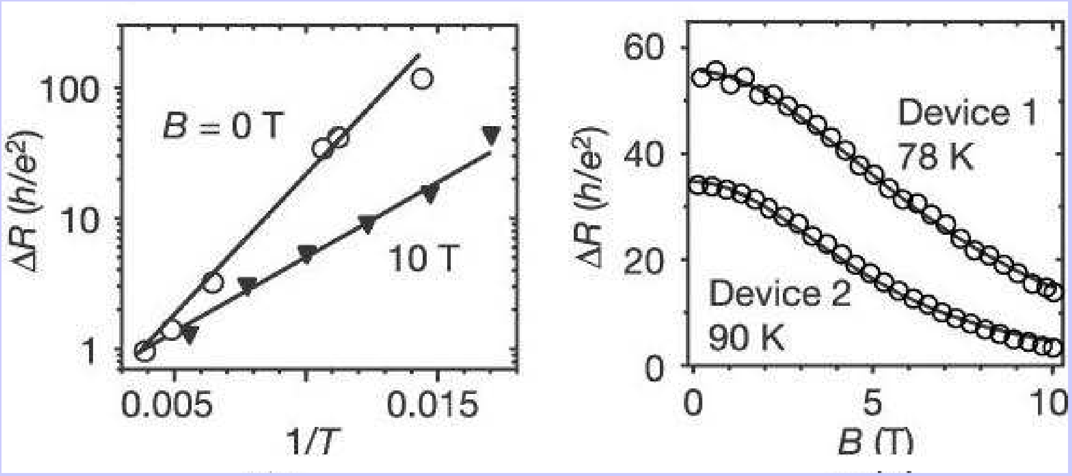

Device 2:

- $\boldsymbol{B} = 0$: $E_g^0 = 40$ meV
  $|t_1|^2 + |t_2|^2 = 1.6$ $\Longrightarrow$ two channels, nearly ballistic transport
- $\boldsymbol{B} = 10$ T : $E_g = 22$ meV
  $|t_1|^2 + |t_2|^2 = 0.8$ $\Longrightarrow$ at least one band is lowered

Thermally activated transport through charge-depleted CNTs

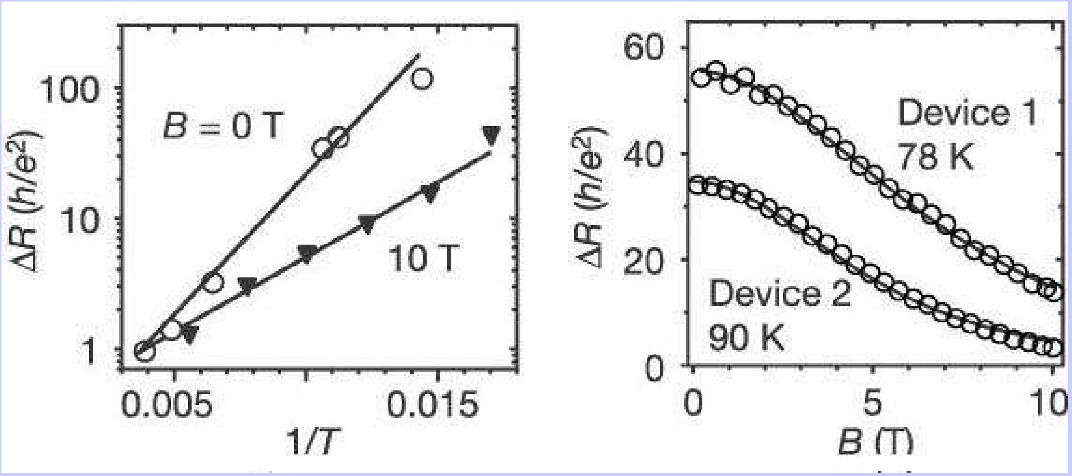

Device 2:

- $\boldsymbol{B}=0$: $E_{\mathrm{g}}^{0}=40$ meV
  $|t_1|^2+|t_2|^2=1.6$ $\Longrightarrow$ two channels, nearly ballistic transport
- $\boldsymbol{B}=10$ T : $E_{\mathrm{g}}=22$ meV
  $|t_1|^2+|t_2|^2=0.8$ $\Longrightarrow$ at least one band is lowered

Device 1 & 2: $\Delta R(B,T=\mathrm{const})$ $\Longrightarrow$ $\mu_{\mathrm{orb}}=\dfrac{a}{2\cos\phi}$

$E_{\mathrm{g}}(B)=E_{\mathrm{g}}^{0}-aB$

Summary of thermal activation results

	D(nm)	E_{g}^{0}(meV)	$\phi(^\circ)$	a(meVT^{-1})	μ_{orb}(meVT^{-1})	
					Experiment	Theory
Device 1	2.6$\pm$0.3	36$\pm$3	30$\pm$3	1.3$\pm$0.1	0.7$\pm$0.1	0.5$\pm$0.1
			60$\pm$3	0.7$\pm$0.1	0.7$\pm$0.1	0.5$\pm$0.1
Device 2	5.0$\pm$0.3	40$\pm$3	45$\pm$3	2.1$\pm$0.2	1.5$\pm$0.2	1.0$\pm$0.2

Energy level spectroscopy near bandgap of CNTQDs

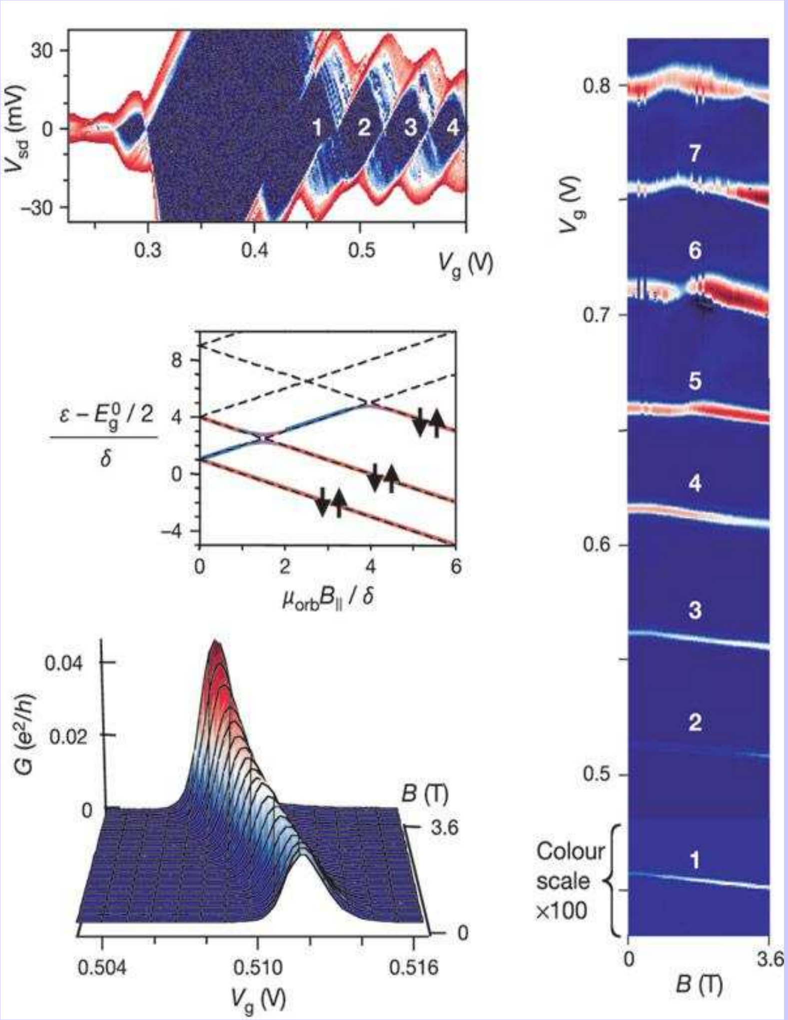

Device 1, T=1.5 K, $\phi = 30°$, $V_g > V^*$:

- p-n-tunnel barriers between suspended and oxide-bound segments

Energy level spectroscopy near bandgap of CNTQDs

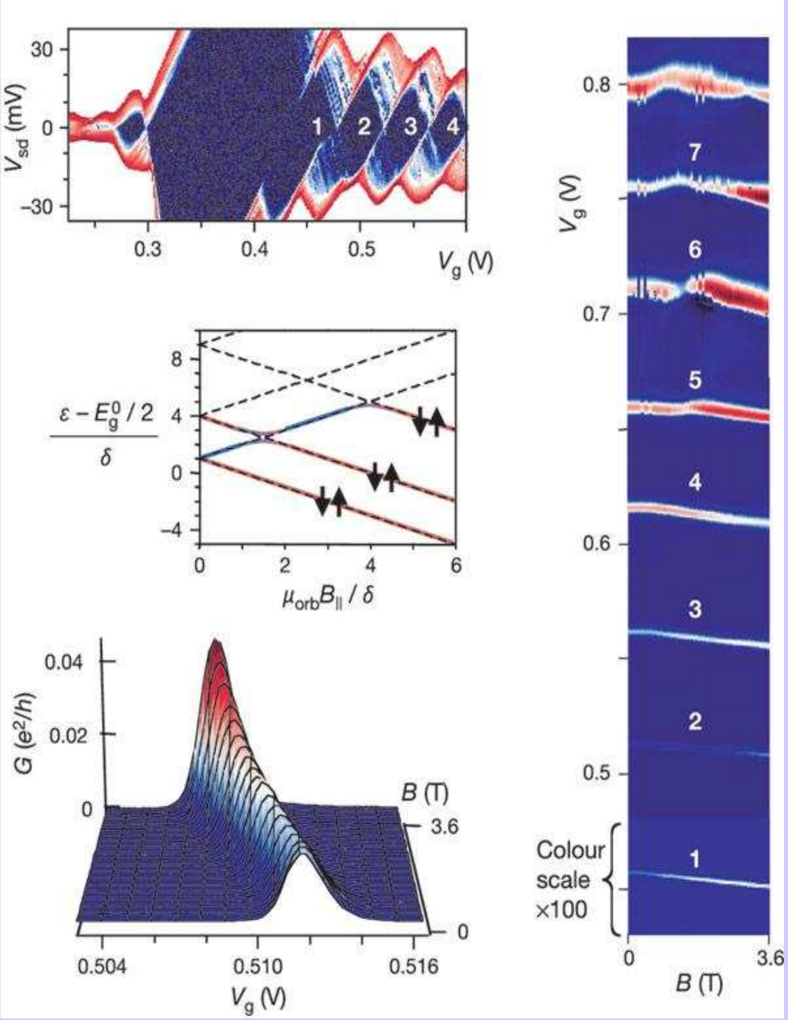

Device 1, T=1.5 K, $\phi = 30°$, $V_g > V^*$:

- p-n-tunnel barriers between suspended and oxide-bound segments
- Quantum levels:

$$\varepsilon(n, i, B_{\|}) = \frac{E_g^0}{2} + \frac{\hbar^2\pi^2}{2m_i^* L^2} n^2 \pm \mu_{\rm orb} B_{\|}$$

Energy level spectroscopy near bandgap of CNTQDs

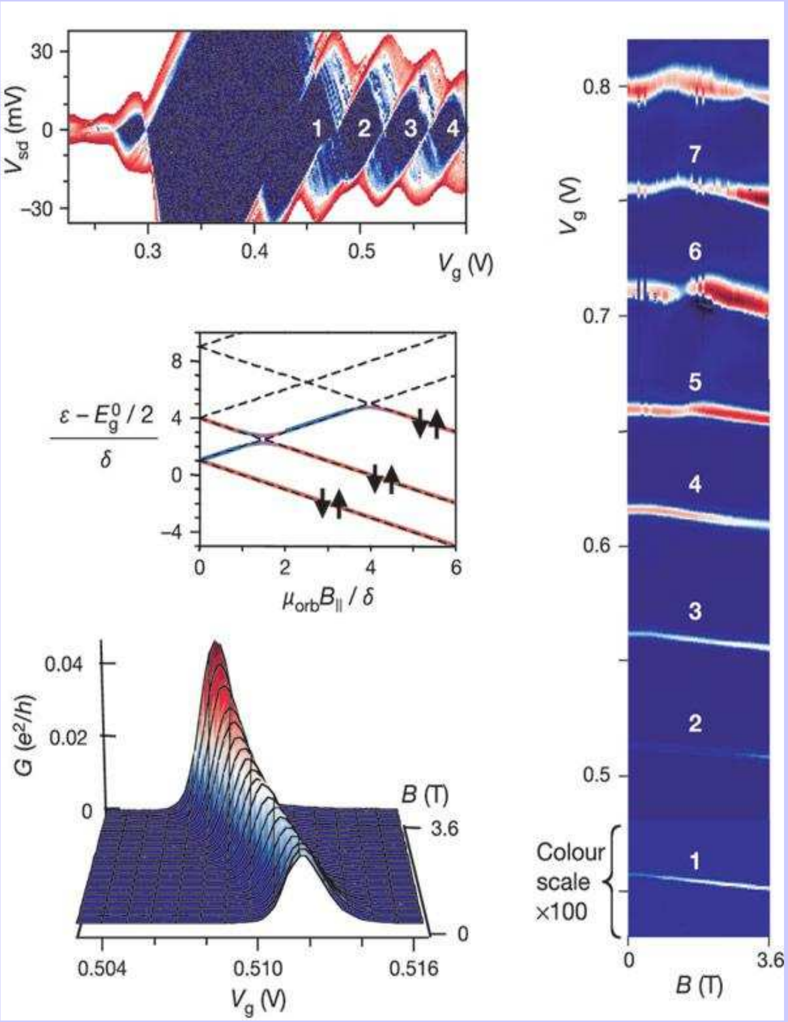

Device 1, T=1.5 K, $\phi = 30°$, $V_\mathrm{g} > V^*$:

- p-n-tunnel barriers between suspended and oxide-bound segments
- Quantum levels:

$$\varepsilon(n, i, B_\|) = \frac{E_\mathrm{g}^0}{2} + \frac{\hbar^2\pi^2}{2m_i^* L^2} n^2 \pm \mu_\mathrm{orb} B_\|$$

- $G(V_\mathrm{g}, B)$, first 8 Coulomb peaks

$\rightarrow$ Break of sub-band degeneracy

$\frac{d\varepsilon}{dB} > 0$ tunnelling in CW-states

$\frac{d\varepsilon}{dB} < 0$ tunnelling in ACW-states

Energy level spectroscopy near bandgap of CNTQDs

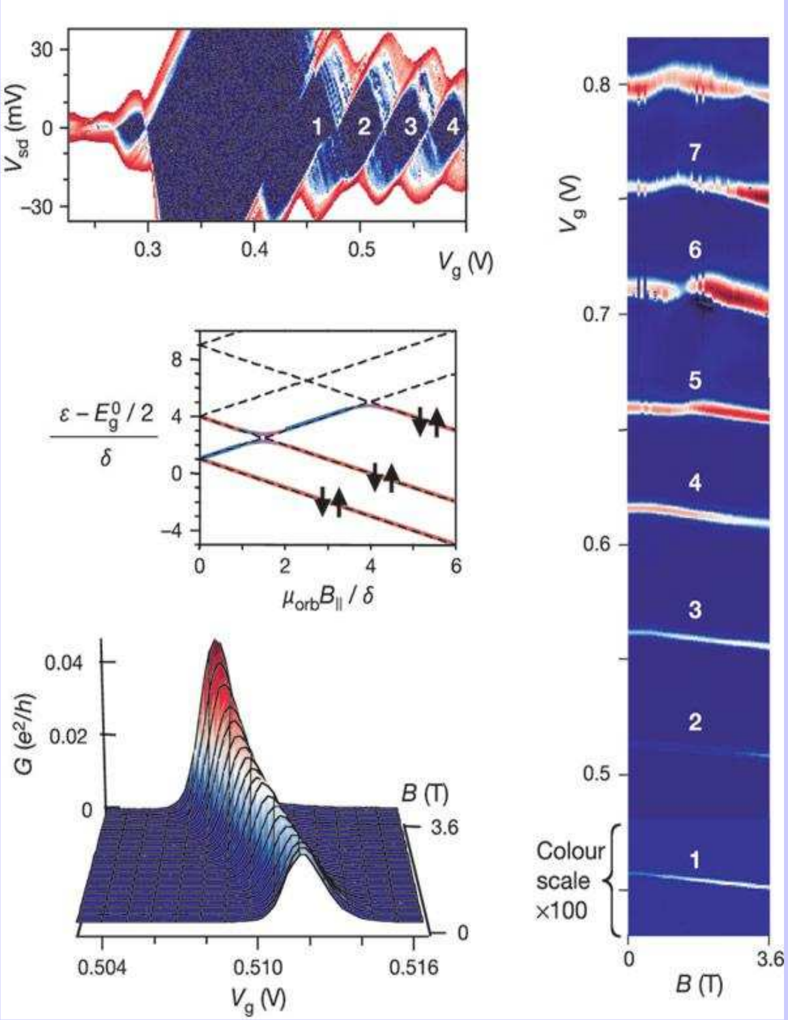

Device 1, T=1.5 K, $\phi = 30°$, $V_{\rm g} > V^*$:

- p-n-tunnel barriers between suspended and oxide-bound segments
- Quantum levels:

$$\varepsilon(n, i, B_{\|}) = \frac{E_{\rm g}^0}{2} + \frac{\hbar^2\pi^2}{2m_i^* L^2} n^2 \pm \mu_{\rm orb} B_{\|}$$

- $G(V_{\rm g}, B)$, first 8 Coulomb peaks

  $\rightarrow$ Break of sub-band degeneracy

  $\frac{d\varepsilon}{dB} > 0$ tunnelling in CW-states

  $\frac{d\varepsilon}{dB} < 0$ tunnelling in ACW-states

- $G(V_{\rm g}, B)$ at 2. Coulomb peak

  $\rightarrow$ Shift $\quad \frac{dV_{\rm g}}{dB} \sim \frac{d\varepsilon}{dB}$

Energy level spectroscopy near bandgap of CNTQDs

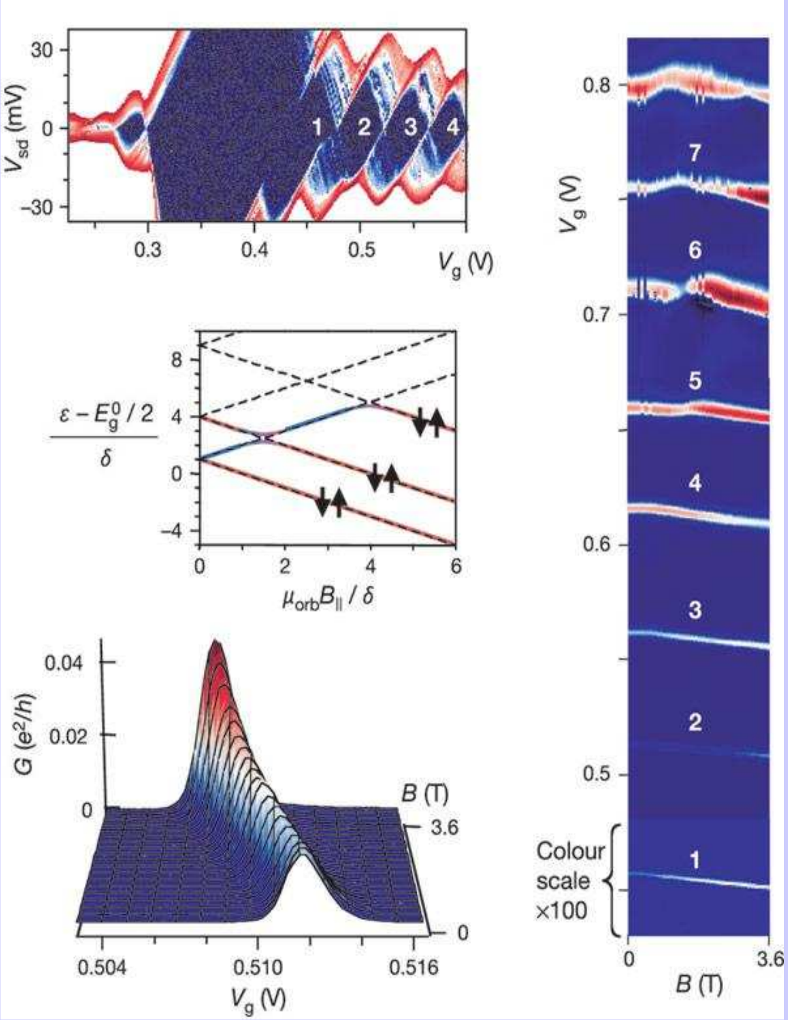

Device 1, T=1.5 K, $\phi = 30°$, $V_\mathrm{g} > V^*$:

- p-n-tunnel barriers between suspended and oxide-bound segments
- Quantum levels:

$$\varepsilon(n, i, B_\|) = \frac{E_\mathrm{g}^0}{2} + \frac{\hbar^2\pi^2}{2m_i^* L^2} n^2 \pm \mu_\mathrm{orb} B_\|$$

- $G(V_\mathrm{g}, B)$, first 8 Coulomb peaks

  $\rightarrow$ Break of sub-band degeneracy

  $\frac{d\varepsilon}{dB} > 0$ tunnelling in CW-states

  $\frac{d\varepsilon}{dB} < 0$ tunnelling in ACW-states

- $G(V_\mathrm{g}, B)$ at 2. Coulomb peak

  $\rightarrow$ Shift $\frac{dV_\mathrm{g}}{dB} \sim \frac{d\varepsilon}{dB}$

$$\Longrightarrow \mu_\mathrm{orb} = \left|\frac{d\varepsilon}{dB}\right| = 0.7 \pm 0.1 \text{ meVT}^{-1}$$

Summary

	$\mu_{\rm orb}$(meVT^{-1})		
	Thermal activation	CNTQDs	Theory
Device 1	0.7±0.1	0.7±0.1	0.5±0.1
Device 2	1.5±0.2		1.0±0.2

- $\longrightarrow$ applied magnetic field split the **K**$_1$ and **K**$_2$ sub-bands
- $\longrightarrow$ measured $\mu_{\rm orb}$ scale with the diameter
- $\longrightarrow$ $\mu_{\rm orb}$ is an order of magnitude larger than the previously measured spin magnetic moments in CNTs